nature physics

SUPPLEMENTARY INFORMATION

DOI: 10.1038/NPHYS1309

Quantum error correction beyond qubits –Supplemental material–

Takao Aoki[1], Go Takahashi[1,2], Tadashi Kajiya[1,2]
Jun-ichi Yoshikawa[1,2], Samuel L. Braunstein[3],
Peter van Loock[4] & Akira Furusawa[1,2]

[1]Department of Applied Physics and Quantum Phase Electronics Center, School of Engineering, The University of Tokyo, 7-3-1 Hongo, Bunkyo-ku, Tokyo 113-8656, Japan
[2]CREST, Japan Science and Technology (JST) Agency, 5, Sanbancho, Chiyoda-ku, Tokyo 102-0075, Japan
[3]Computer Science, University of York, York YO10 5DD, UK
[4]Optical Quantum Information Theory Group, Max Planck Institute for the Science of Light and Institute of Theoretical Physics I, Universität Erlangen-Nürnberg, Staudtstr.7/B2, 91058 Erlangen, Germany

APPENDIX A: ENCODING

Equation (1) describes a nine-port device acting upon the signal input mode, two x-squeezed ancilla modes ("an1" and "an4" in Fig. 1 of main body), and six p-squeezed ancilla modes ("an2", "an3", "an5", "an6", "an7", and "an8" in Fig. 1). Labeling the nine input modes by subscripts one through nine, we obtain the output quadrature operators of the encoded state,

$$
\begin{aligned}
\hat{x}_1 &= \frac{1}{3}\hat{x}_{\rm in} + \frac{\sqrt{2}}{3}\hat{x}^{(0)}_{\rm an1}e^{-r_1} + \sqrt{\frac{2}{3}}\hat{x}^{(0)}_{\rm an2}e^{r_2},\\
\hat{p}_1 &= \frac{1}{3}\hat{p}_{\rm in} + \frac{\sqrt{2}}{3}\hat{p}^{(0)}_{\rm an1}e^{r_1} + \sqrt{\frac{2}{3}}\hat{p}^{(0)}_{\rm an2}e^{-r_2},\\
\hat{x}_2 &= \frac{1}{3}\hat{x}_{\rm in} + \frac{\sqrt{2}}{3}\hat{x}^{(0)}_{\rm an1}e^{-r_1} - \sqrt{\frac{1}{6}}\hat{x}^{(0)}_{\rm an2}e^{r_2}\\
&\quad + \sqrt{\frac{1}{2}}\hat{x}^{(0)}_{\rm an3}e^{r_3},\\
\hat{p}_2 &= \frac{1}{3}\hat{p}_{\rm in} + \frac{\sqrt{2}}{3}\hat{p}^{(0)}_{\rm an1}e^{r_1} - \sqrt{\frac{1}{6}}\hat{p}^{(0)}_{\rm an2}e^{-r_2}\\
&\quad + \sqrt{\frac{1}{2}}\hat{p}^{(0)}_{an3}e^{-r_3},\\
\hat{x}_3 &= \frac{1}{3}\hat{x}_{\rm in} + \frac{\sqrt{2}}{3}\hat{x}^{(0)}_{\rm an1}e^{-r_1} - \sqrt{\frac{1}{6}}\hat{x}^{(0)}_{\rm an2}e^{r_2}\\
&\quad - \sqrt{\frac{1}{2}}\hat{x}^{(0)}_{\rm an3}e^{r_3},\\
\hat{p}_3 &= \frac{1}{3}\hat{p}_{\rm in} + \frac{\sqrt{2}}{3}\hat{p}^{(0)}_{\rm an1}e^{r_1} - \sqrt{\frac{1}{6}}\hat{p}^{(0)}_{\rm an2}e^{-r_2}\\
&\quad - \sqrt{\frac{1}{2}}\hat{p}^{(0)}_{\rm an3}e^{-r_3},\\
\hat{x}_4 &= \frac{1}{3}\hat{x}_{\rm in} - \frac{1}{3\sqrt{2}}\hat{x}^{(0)}_{\rm an1}e^{-r_1} + \sqrt{\frac{1}{6}}\hat{x}^{(0)}_{\rm an4}e^{-r_4}\\
&\quad + \sqrt{\frac{2}{3}}\hat{x}^{(0)}_{\rm an5}e^{r_5},\\
\hat{p}_4 &= \frac{1}{3}\hat{p}_{\rm in} - \frac{1}{3\sqrt{2}}\hat{p}^{(0)}_{\rm an1}e^{r_1} + \sqrt{\frac{1}{6}}\hat{p}^{(0)}_{\rm an4}e^{r_4}\\
&\quad + \sqrt{\frac{2}{3}}\hat{p}^{(0)}_{\rm an5}e^{-r_5},\\
\hat{x}_5 &= \frac{1}{3}\hat{x}_{\rm in} - \frac{1}{3\sqrt{2}}\hat{x}^{(0)}_{\rm an1}e^{-r_1} + \sqrt{\frac{1}{6}}\hat{x}^{(0)}_{an4}e^{-r_4}\\
&\quad - \sqrt{\frac{1}{6}}\hat{x}^{(0)}_{\rm an5}e^{r_5} + \sqrt{\frac{1}{2}}\hat{x}^{(0)}_{\rm an6}e^{r_6},\\
\hat{p}_5 &= \frac{1}{3}\hat{p}_{\rm in} - \frac{1}{3\sqrt{2}}\hat{p}^{(0)}_{\rm an1}e^{r_1} + \sqrt{\frac{1}{6}}\hat{p}^{(0)}_{\rm an4}e^{r_4}\\
&\quad - \sqrt{\frac{1}{6}}\hat{p}^{(0)}_{\rm an5}e^{-r_5} + \sqrt{\frac{1}{2}}\hat{p}^{(0)}_{\rm an6}e^{-r_6},\\
\hat{x}_6 &= \frac{1}{3}\hat{x}_{\rm in} - \frac{1}{3\sqrt{2}}\hat{x}^{(0)}_{\rm an1}e^{-r_1} + \sqrt{\frac{1}{6}}\hat{x}^{(0)}_{\rm an4}e^{-r_4}\\
&\quad - \sqrt{\frac{1}{6}}\hat{x}^{(0)}_{\rm an5}e^{r_5} - \sqrt{\frac{1}{2}}\hat{x}^{(0)}_{\rm an6}e^{r_6},\\
\hat{p}_6 &= \frac{1}{3}\hat{p}_{\rm in} - \frac{1}{3\sqrt{2}}\hat{p}^{(0)}_{\rm an1}e^{r_1} + \sqrt{\frac{1}{6}}\hat{p}^{(0)}_{\rm an4}e^{r_4}\\
&\quad - \sqrt{\frac{1}{6}}\hat{p}^{(0)}_{\rm an5}e^{-r_5} - \sqrt{\frac{1}{2}}\hat{p}^{(0)}_{\rm an6}e^{-r_6},\\
\hat{x}_7 &= \frac{1}{3}\hat{x}_{\rm in} - \frac{1}{3\sqrt{2}}\hat{x}^{(0)}_{\rm an1}e^{-r_1}\\
&\quad - \sqrt{\frac{1}{6}}\hat{x}^{(0)}_{\rm an4}e^{-r_4} + \sqrt{\frac{2}{3}}\hat{x}^{(0)}_{\rm an7}e^{r_7},\\
\hat{p}_7 &= \frac{1}{3}\hat{p}_{\rm in} - \frac{1}{3\sqrt{2}}\hat{p}^{(0)}_{\rm an1}e^{r_1} - \sqrt{\frac{1}{6}}\hat{p}^{(0)}_{\rm an4}e^{r_4}\\
&\quad + \sqrt{\frac{2}{3}}\hat{p}^{(0)}_{\rm an7}e^{-r_7},\\
\hat{x}_8 &= \frac{1}{3}\hat{x}_{\rm in} - \frac{1}{3\sqrt{2}}\hat{x}^{(0)}_{\rm an1}e^{-r_1} - \sqrt{\frac{1}{6}}\hat{x}^{(0)}_{\rm an4}e^{-r_4}\\
&\quad - \sqrt{\frac{1}{6}}\hat{x}^{(0)}_{\rm an7}e^{r_7} + \sqrt{\frac{1}{2}}\hat{x}^{(0)}_{\rm an8}e^{r_8},\\
\hat{p}_8 &= \frac{1}{3}\hat{p}_{\rm in} - \frac{1}{3\sqrt{2}}\hat{p}^{(0)}_{\rm an1}e^{r_1} - \sqrt{\frac{1}{6}}\hat{p}^{(0)}_{\rm an4}e^{r_4}\\
&\quad - \sqrt{\frac{1}{6}}\hat{p}^{(0)}_{\rm an7}e^{-r_7} + \sqrt{\frac{1}{2}}\hat{p}^{(0)}_{\rm an8}e^{-r_8},\\
\hat{x}_9 &= \frac{1}{3}\hat{x}_{\rm in} - \frac{1}{3\sqrt{2}}\hat{x}^{(0)}_{\rm an1}e^{-r_1} - \sqrt{\frac{1}{6}}\hat{x}^{(0)}_{\rm an4}e^{-r_4}\\
&\quad - \sqrt{\frac{1}{6}}\hat{x}^{(0)}_{\rm an7}e^{r_7} - \sqrt{\frac{1}{2}}\hat{x}^{(0)}_{\rm an8}e^{r_8},\\
\hat{p}_9 &= \frac{1}{3}\hat{p}_{\rm in} - \frac{1}{3\sqrt{2}}\hat{p}^{(0)}_{\rm an1}e^{r_1} - \sqrt{\frac{1}{6}}\hat{p}^{(0)}_{\rm an4}e^{r_4}\\
&\quad - \sqrt{\frac{1}{6}}\hat{p}^{(0)}_{\rm an7}e^{-r_7} - \sqrt{\frac{1}{2}}\hat{p}^{(0)}_{\rm an8}e^{-r_8}. \qquad \text{(A1)}
\end{aligned}
$$

Note that with respect to these subscripts, eq. (1) can be expressed by $T_{789}T_{456}T_{123}T_{147}$ for modes 1 (signal input), 2 ("an2"), 3 ("an3"), 4 ("an1"), 5 ("an5"), 6 ("an6"), 7

DOI: 10.1038/NPHYS1309

("an4"), 8 ("an7"), and 9 ("an8").

The encoded state exhibits the following quadrature quantum correlations in the case of nonzero squeezing,

$$\begin{aligned}
\hat{x}_1+\hat{x}_2+\hat{x}_3-(\hat{x}_4+\hat{x}_5+\hat{x}_6) &= \frac{3}{\sqrt{2}}\hat{x}^{(0)}_{\mathrm{an1}}e^{-r_1}-\sqrt{\frac{3}{2}}\hat{x}^{(0)}_{\mathrm{an4}}e^{-r_4},\\
\hat{x}_4+\hat{x}_5+\hat{x}_6-(\hat{x}_7+\hat{x}_8+\hat{x}_9) &= \sqrt{6}\hat{x}^{(0)}_{\mathrm{an4}}e^{-r_4},\\
\hat{p}_1-\hat{p}_2 &= \sqrt{\frac{3}{2}}\hat{p}^{(0)}_{\mathrm{an2}}e^{-r_2}-\frac{1}{\sqrt{2}}\hat{p}^{(0)}_{\mathrm{an3}}e^{-r_3},\\
\hat{p}_2-\hat{p}_3 &= \sqrt{2}\hat{p}^{(0)}_{\mathrm{an3}}e^{-r_3},\\
\hat{p}_4-\hat{p}_5 &= \sqrt{\frac{3}{2}}\hat{p}^{(0)}_{\mathrm{an5}}e^{-r_5}-\frac{1}{\sqrt{2}}\hat{p}^{(0)}_{\mathrm{an6}}e^{-r_6},\\
\hat{p}_5-\hat{p}_6 &= \sqrt{2}\hat{p}^{(0)}_{\mathrm{an6}}e^{-r_6},\\
\hat{p}_7-\hat{p}_8 &= \sqrt{\frac{3}{2}}\hat{p}^{(0)}_{\mathrm{an7}}e^{-r_7}-\frac{1}{\sqrt{2}}\hat{p}^{(0)}_{\mathrm{an8}}e^{-r_8},\\
\hat{p}_8-\hat{p}_9 &= \sqrt{2}\hat{p}^{(0)}_{\mathrm{an8}}e^{-r_8}.
\end{aligned} \tag{A2}$$

In the limit $r_{1-8}\to\infty$, the quadrature operators become perfectly correlated,

$$\begin{aligned}
\hat{x}_1+\hat{x}_2+\hat{x}_3 &= \hat{x}_4+\hat{x}_5+\hat{x}_6=\hat{x}_7+\hat{x}_8+\hat{x}_9,\\
\hat{p}_1 &= \hat{p}_2=\hat{p}_3,\\
\hat{p}_4 &= \hat{p}_5=\hat{p}_6,\\
\hat{p}_7 &= \hat{p}_8=\hat{p}_9.
\end{aligned} \tag{A3}$$

These correlations are analogous expressions to the eight stabilizer conditions of the Shor qubit code (where for continuous variables, Pauli operators are replaced by Weyl-Heisenberg phase-space operators). Note that these correlations hold for *any* signal input state, i.e., for any resulting "code words", again similar to the stabilizer conditions for qubits. In order to obtain a sufficient set of entanglement witnesses for verifying a fully inseparable nine-party state, additional quadrature correlations must be considered; these extra correlations are expressed in terms of the "logical" quadratures in the code space which depend also on the signal state (see appendix E).

APPENDIX B: DECODING AND CORRECTION

Random phase fluctuations are transferred onto one selected beam of the encoded state, leading to random phase-space displacements of one of the nine optical modes. This effect can be described by adding error quadrature operators to the corresponding mode k, $\lambda_k\hat{x}^e_k$ and $\lambda_k\hat{p}^e_k$, where the parameter λ_k will be set to one for the single mode of the noisy quantum channel and otherwise chosen to be zero. After the decoding step, $T^{-1}_{147}T^{-1}_{123}T^{-1}_{456}T^{-1}_{789}$, the outgoing quadrature operators become

$$\begin{aligned}
\hat{x}'_1 &= \hat{x}_{\mathrm{in}}+\frac{1}{3}\sum_{k=1}^{9}\lambda_k\hat{x}^e_k,\\
\hat{p}'_1 &= \hat{p}_{\mathrm{in}}+\frac{1}{3}\sum_{k=1}^{9}\lambda_k\hat{p}^e_k,\\
\hat{x}'_2 &= \hat{x}^{(0)}_{\mathrm{an2}}e^{r_2}+\sqrt{\frac{2}{3}}\lambda_1\hat{x}^e_1-\frac{1}{\sqrt{6}}\left(\lambda_2\hat{x}^e_2+\lambda_3\hat{x}^e_3\right),\\
\hat{p}'_2 &= \hat{p}^{(0)}_{\mathrm{an2}}e^{-r_2}+\sqrt{\frac{2}{3}}\lambda_1\hat{p}^e_1-\frac{1}{\sqrt{6}}\left(\lambda_2\hat{p}^e_2+\lambda_3\hat{p}^e_3\right),\\
\hat{x}'_3 &= \hat{x}^{(0)}_{\mathrm{an3}}e^{r_3}+\frac{1}{\sqrt{2}}\left(\lambda_2\hat{x}^e_2-\lambda_3\hat{x}^e_3\right),\\
\hat{p}'_3 &= \hat{p}^{(0)}_{\mathrm{an3}}e^{-r_3}+\frac{1}{\sqrt{2}}\left(\lambda_2\hat{p}^e_2-\lambda_3\hat{p}^e_3\right),\\
\hat{x}'_4 &= \hat{x}^{(0)}_{\mathrm{an1}}e^{-r_1}+\frac{\sqrt{2}}{3}\sum_{k=1}^{3}\lambda_k\hat{x}^e_k-\frac{1}{\sqrt{18}}\sum_{k=4}^{9}\lambda_k\hat{x}^e_k,\\
\hat{p}'_4 &= \hat{p}^{(0)}_{\mathrm{an1}}e^{r_1}+\frac{\sqrt{2}}{3}\sum_{k=1}^{3}\lambda_k\hat{p}^e_k-\frac{1}{\sqrt{18}}\sum_{k=4}^{9}\lambda_k\hat{p}^e_k,\\
\hat{x}'_5 &= \hat{x}^{(0)}_{\mathrm{an5}}e^{r_5}+\sqrt{\frac{2}{3}}\lambda_4\hat{x}^e_4-\frac{1}{\sqrt{6}}\left(\lambda_5\hat{x}^e_5+\lambda_6\hat{x}^e_6\right),\\
\hat{p}'_5 &= \hat{p}^{(0)}_{\mathrm{an5}}e^{-r_5}+\sqrt{\frac{2}{3}}\lambda_4\hat{p}^e_4-\frac{1}{\sqrt{6}}\left(\lambda_5\hat{p}^e_5+\lambda_6\hat{p}^e_6\right),\\
\hat{x}'_6 &= \hat{x}^{(0)}_{\mathrm{an6}}e^{r_6}+\frac{1}{\sqrt{2}}\left(\lambda_5\hat{x}^e_5-\lambda_6\hat{x}^e_6\right),\\
\hat{p}'_6 &= \hat{p}^{(0)}_{\mathrm{an6}}e^{-r_6}+\frac{1}{\sqrt{2}}\left(\lambda_5\hat{p}^e_5-\lambda_6\hat{p}^e_6\right),\\
\hat{x}'_7 &= \hat{x}^{(0)}_{\mathrm{an4}}e^{-r_4}+\frac{1}{\sqrt{6}}\left(\sum_{k=4}^{6}\lambda_k\hat{x}^e_k-\sum_{k=7}^{9}\lambda_k\hat{x}^e_k\right),\\
\hat{p}'_7 &= \hat{p}^{(0)}_{\mathrm{an4}}e^{r_4}+\frac{1}{\sqrt{6}}\left(\sum_{k=4}^{6}\lambda_k\hat{p}^e_k-\sum_{k=7}^{9}\lambda_k\hat{p}^e_k\right),\\
\hat{x}'_8 &= \hat{x}^{(0)}_{\mathrm{an7}}e^{r_7}+\sqrt{\frac{2}{3}}\lambda_7\hat{x}^e_7-\frac{1}{\sqrt{6}}\left(\lambda_8\hat{x}^e_8+\lambda_9\hat{x}^e_9\right),\\
\hat{p}'_8 &= \hat{p}^{(0)}_{\mathrm{an7}}e^{-r_7}+\sqrt{\frac{2}{3}}\lambda_7\hat{p}^e_7-\frac{1}{\sqrt{6}}\left(\lambda_8\hat{p}^e_8+\lambda_9\hat{p}^e_9\right),\\
\hat{x}'_9 &= \hat{x}^{(0)}_{\mathrm{an8}}e^{r_8}+\frac{1}{\sqrt{2}}\left(\lambda_8\hat{x}^e_8-\lambda_9\hat{x}^e_9\right),\\
\hat{p}'_9 &= \hat{p}^{(0)}_{\mathrm{an8}}e^{-r_8}+\frac{1}{\sqrt{2}}\left(\lambda_8\hat{p}^e_8-\lambda_9\hat{p}^e_9\right).
\end{aligned} \tag{B1}$$

Modes two through nine are measured via suitable homodyne detectors, i.e., the local oscillator phase is adjusted to detect those quadratures which are quiet if there was no error. After the corresponding feedforward operations on the first mode, the signal input state will be recovered in mode 1 up to the finite squeezing from the ancilla modes.

For example, in the case of an error transferred onto mode 1, $\lambda_k = \delta_{k1}$,

$$\begin{aligned} \hat{x}_1' &= \hat{x}_{\rm in} + \frac{1}{3}\hat{x}_1^e, \\ \hat{p}_1' &= \hat{p}_{\rm in} + \frac{1}{3}\hat{p}_1^e, \end{aligned} \tag{B2}$$

only for detectors 1 and 2 (see Fig. 2 of main body), measuring $\hat{x}_4'$ (position of "an1") and $\hat{p}_2'$ (momentum of "an2"), respectively, results clearly different from zero (coming from the error) are obtained. All the remaining detectors show results around zero. In order to correct the error, mode 1 is displaced according to

$$\begin{aligned} \hat{x}_1' &\rightarrow \hat{x}_1' - \frac{1}{\sqrt{2}}\hat{x}_4', \\ \hat{p}_1' &\rightarrow \hat{p}_1' - \frac{1}{\sqrt{6}}\hat{p}_2', \end{aligned} \tag{B3}$$

leading to

$$\begin{aligned} \hat{x}_{\rm out} &= \hat{x}_{\rm in} - \frac{1}{\sqrt{2}}\hat{x}_{\rm an1}^{(0)} e^{-r_1}, \\ \hat{p}_{\rm out} &= \hat{p}_{\rm in} - \frac{1}{\sqrt{6}}\hat{p}_{\rm an2}^{(0)} e^{-r_2}, \end{aligned} \tag{B4}$$

using eqs. (B1).

Similarly, in the case of an error transferred onto mode 9, $\lambda_k = \delta_{k9}$, we have

$$\begin{aligned} \hat{x}_1' &= \hat{x}_{\rm in} + \frac{1}{3}\hat{x}_9^e, \\ \hat{p}_1' &= \hat{p}_{\rm in} + \frac{1}{3}\hat{p}_9^e. \end{aligned} \tag{B5}$$

Now the only nonzero outputs occur at detectors 1 and 4 (Fig. 2), measuring $\hat{x}_4'$ (position of "an1") and $\hat{x}_7'$ (position of "an4"), respectively, and at detectors 7 and 8, measuring $\hat{p}_8'$ (momentum of "an7") and $\hat{p}_9'$ (momentum of "an8"), respectively. Possible correction displacements are

$$\begin{aligned} \hat{x}_1' &\rightarrow \hat{x}_1' + \sqrt{2}\hat{x}_4', \\ \hat{x}_1' &\rightarrow \hat{x}_1' + \sqrt{\frac{2}{3}}\hat{x}_7', \end{aligned} \tag{B6}$$

for x, and

$$\begin{aligned} \hat{p}_1' &\rightarrow \hat{p}_1' + \sqrt{\frac{2}{3}}\hat{p}_8', \\ \hat{p}_1' &\rightarrow \hat{p}_1' + \frac{\sqrt{2}}{3}\hat{p}_9', \end{aligned} \tag{B7}$$

for p. These corrections result in the output quadratures

$$\begin{aligned} \hat{x}_{\rm out} &= \hat{x}_{\rm in} + \sqrt{2}\hat{x}_{\rm an1}^{(0)} e^{-r_1}, \\ \hat{x}_{\rm out} &= \hat{x}_{\rm in} + \sqrt{\frac{2}{3}}\hat{x}_{\rm an4}^{(0)} e^{-r_4}, \\ \hat{p}_{\rm out} &= \hat{p}_{\rm in} + \sqrt{\frac{2}{3}}\hat{p}_{\rm an7}^{(0)} e^{-r_7}, \\ \hat{p}_{\rm out} &= \hat{p}_{\rm in} + \frac{\sqrt{2}}{3}\hat{p}_{\rm an8}^{(0)} e^{-r_8}, \end{aligned} \tag{B8}$$

always nearly recovering the signal input state.

Similar calculations yield the quadrature operators for the output state of mode 1 after the error correction protocol in the case of an error on modes two through eight; for an error on mode 2,

$$\begin{aligned} \hat{x}_{\rm out,det1} &= \hat{x}_{\rm in} - \frac{1}{\sqrt{2}}\hat{x}_{\rm an1}^{(0)} e^{-r_1}, \\ \hat{p}_{\rm out,det2} &= \hat{p}_{\rm in} + \sqrt{\frac{2}{3}}\hat{p}_{\rm an2}^{(0)} e^{-r_2}, \\ \hat{p}_{\rm out,det3} &= \hat{p}_{\rm in} - \frac{\sqrt{2}}{3}\hat{p}_{\rm an3}^{(0)} e^{-r_3}, \end{aligned} \tag{B9}$$

for an error on mode 3,

$$\begin{aligned} \hat{x}_{\rm out,det1} &= \hat{x}_{\rm in} - \frac{1}{\sqrt{2}}\hat{x}_{\rm an1}^{(0)} e^{-r_1}, \\ \hat{p}_{\rm out,det2} &= \hat{p}_{\rm in} + \sqrt{\frac{2}{3}}\hat{p}_{\rm an2}^{(0)} e^{-r_2}, \\ \hat{p}_{\rm out,det3} &= \hat{p}_{\rm in} + \frac{\sqrt{2}}{3}\hat{p}_{\rm an3}^{(0)} e^{-r_3}, \end{aligned} \tag{B10}$$

for an error on mode 4,

$$\begin{aligned} \hat{x}_{\rm out,det1} &= \hat{x}_{\rm in} + \sqrt{2}\hat{x}_{\rm an1}^{(0)} e^{-r_1}, \\ \hat{x}_{\rm out,det4} &= \hat{x}_{\rm in} - \sqrt{\frac{2}{3}}\hat{x}_{\rm an4}^{(0)} e^{-r_4}, \\ \hat{p}_{\rm out,det5} &= \hat{p}_{\rm in} - \frac{1}{\sqrt{6}}\hat{p}_{\rm an5}^{(0)} e^{-r_5}, \end{aligned} \tag{B11}$$

for an error on mode 5,

$$\begin{aligned} \hat{x}_{\rm out,det1} &= \hat{x}_{\rm in} + \sqrt{2}\hat{x}_{\rm an1}^{(0)} e^{-r_1}, \\ \hat{x}_{\rm out,det4} &= \hat{x}_{\rm in} - \sqrt{\frac{2}{3}}\hat{x}_{\rm an4}^{(0)} e^{-r_4}, \\ \hat{p}_{\rm out,det5} &= \hat{p}_{\rm in} - \sqrt{\frac{2}{3}}\hat{p}_{\rm an5}^{(0)} e^{-r_5}, \\ \hat{p}_{\rm out,det6} &= \hat{p}_{\rm in} - \frac{\sqrt{2}}{3}\hat{p}_{\rm an6}^{(0)} e^{-r_6}, \end{aligned} \tag{B12}$$

DOI: 10.1038/NPHYS1309

for an error on mode 6,

$$\begin{aligned}\hat{x}_{\mathrm{out,det1}} &= \hat{x}_{\mathrm{in}} + \sqrt{2}\hat{x}^{(0)}_{\mathrm{an1}}e^{-r_1},\\ \hat{x}_{\mathrm{out,det4}} &= \hat{x}_{\mathrm{in}} - \sqrt{\frac{2}{3}}\hat{x}^{(0)}_{\mathrm{an4}}e^{-r_4},\\ \hat{p}_{\mathrm{out,det5}} &= \hat{p}_{\mathrm{in}} + \sqrt{\frac{2}{3}}\hat{p}^{(0)}_{\mathrm{an5}}e^{-r_5},\\ \hat{p}_{\mathrm{out,det6}} &= \hat{p}_{\mathrm{in}} + \frac{\sqrt{2}}{3}\hat{p}^{(0)}_{\mathrm{an6}}e^{-r_6}, \end{aligned} \tag{B13}$$

for an error on mode 7,

$$\begin{aligned}\hat{x}_{\mathrm{out,det1}} &= \hat{x}_{\mathrm{in}} + \sqrt{2}\hat{x}^{(0)}_{\mathrm{an1}}e^{-r_1},\\ \hat{x}_{\mathrm{out,det4}} &= \hat{x}_{\mathrm{in}} + \sqrt{\frac{2}{3}}\hat{x}^{(0)}_{\mathrm{an4}}e^{-r_4},\\ \hat{p}_{\mathrm{out,det7}} &= \hat{p}_{\mathrm{in}} - \frac{1}{\sqrt{6}}\hat{p}^{(0)}_{\mathrm{an7}}e^{-r_7}, \end{aligned} \tag{B14}$$

for an error on mode 8,

$$\begin{aligned}\hat{x}_{\mathrm{out,det1}} &= \hat{x}_{\mathrm{in}} + \sqrt{2}\hat{x}^{(0)}_{\mathrm{an1}}e^{-r_1},\\ \hat{x}_{\mathrm{out,det4}} &= \hat{x}_{\mathrm{in}} + \sqrt{\frac{2}{3}}\hat{x}^{(0)}_{\mathrm{an4}}e^{-r_4},\\ \hat{p}_{\mathrm{out,det7}} &= \hat{p}_{\mathrm{in}} + \sqrt{\frac{2}{3}}\hat{p}^{(0)}_{\mathrm{an7}}e^{-r_7},\\ \hat{p}_{\mathrm{out,det8}} &= \hat{p}_{\mathrm{in}} - \frac{\sqrt{2}}{3}\hat{p}^{(0)}_{\mathrm{an8}}e^{-r_8}. \end{aligned} \tag{B15}$$

The additional subscripts "det1", etc., indicate which detector outcomes are used for the correction displacements. These detectors (see Fig. 2) measure the quadratures $\hat{x}'_4$ ("det1"), $\hat{p}'_2$ ("det2"), $\hat{p}'_3$ ("det3"), $\hat{x}'_7$ ("det4"), $\hat{p}'_5$ ("det5"), $\hat{p}'_6$ ("det6"), $\hat{p}'_8$ ("det7"), and $\hat{p}'_9$ ("det8").

Because of the freedom in choosing the correction displacements, there is always an optimal feedforward operation. For example, in the case of an error on mode 2,

$$\begin{aligned}\hat{x}_{\mathrm{out}} &= \hat{x}_{\mathrm{in}} - \frac{1}{\sqrt{2}}\hat{x}^{(0)}_{\mathrm{an1}}e^{-r_1},\\ \hat{p}_{\mathrm{out,det2}} &= \hat{p}_{\mathrm{in}} + \sqrt{\frac{2}{3}}\hat{p}^{(0)}_{\mathrm{an2}}e^{-r_2},\\ \hat{p}_{\mathrm{out,det3}} &= \hat{p}_{\mathrm{in}} - \frac{\sqrt{2}}{3}\hat{p}^{(0)}_{\mathrm{an3}}e^{-r_3}, \end{aligned} \tag{B16}$$

we obtain the following excess noise for the output state,

$$\begin{aligned}\langle(\hat{x}_{\mathrm{out}})^2\rangle &= \langle(\hat{x}_{\mathrm{in}})^2\rangle + \frac{1}{2}\cdot\frac{1}{4}e^{-2r_1},\\ \langle(\hat{p}_{\mathrm{out,det2}})^2\rangle &= \langle(\hat{p}_{\mathrm{in}})^2\rangle + \frac{2}{3}\cdot\frac{1}{4}e^{-2r_2},\\ \langle(\hat{p}_{\mathrm{out,det3}})^2\rangle &= \langle(\hat{p}_{\mathrm{in}})^2\rangle + \frac{2}{9}\cdot\frac{1}{4}e^{-2r_3}. \end{aligned} \tag{B17}$$

However, for $r_2 = r_3 = r$, the optimal feedforward operation leads to

$$\hat{p}_{\mathrm{out,opt}} = \hat{p}_{\mathrm{in}} + \frac{1}{2\sqrt{6}}\hat{p}^{(0)}_{\mathrm{an2}}e^{-r} - \frac{\sqrt{2}}{4}\hat{p}^{(0)}_{\mathrm{an3}}e^{-r}, \tag{B18}$$

corresponding to

$$\langle(\hat{p}_{\mathrm{out,opt}})^2\rangle = \langle(\hat{p}_{\mathrm{in}})^2\rangle + \frac{1}{6}\cdot\frac{1}{4}e^{-2r}, \tag{B19}$$

which is the same as for the case of an error on mode 1. For unequal squeezing, $r_2 \neq r_3$, the optimal feedforward depends on the squeezing values. Therefore, in the current experiment, we use only the output of detector 3 for the feedforward. Table B shows which outputs of the homodyne detectors are used for error correction.

TABLE I: Homodyne detector outputs for feedforward in the current experiments.

channel with an error	quadrature	detectors for feedforward
1	x	1
	p	2
2	x	1
	p	3
3	x	1
	p	3
4	x	4
	p	5
5	x	4
	p	6
6	x	4
	p	6
7	x	4
	p	7
8	x	4
	p	8
9	x	4
	p	8

APPENDIX C: RESULTS OF ERROR SYNDROME MEASUREMENTS

Fig. 1 shows error syndrome measurement results. Here, the input state is a vacuum state. This case is also described in the main body of the paper. A random displacement error in phase space is transferred onto quantum channels one through nine for A-I, respectively. With Table 1 in the main body of the paper and Fig. 1 here, we can decide which quantum channel is subject to an error and derive a corresponding feedforward operation to correct the error.

APPENDIX D: RESULTS OF ERROR CORRECTION

Fig. 2 shows the results of error correction. The results are summarized in Table 2 in the main body of the paper.

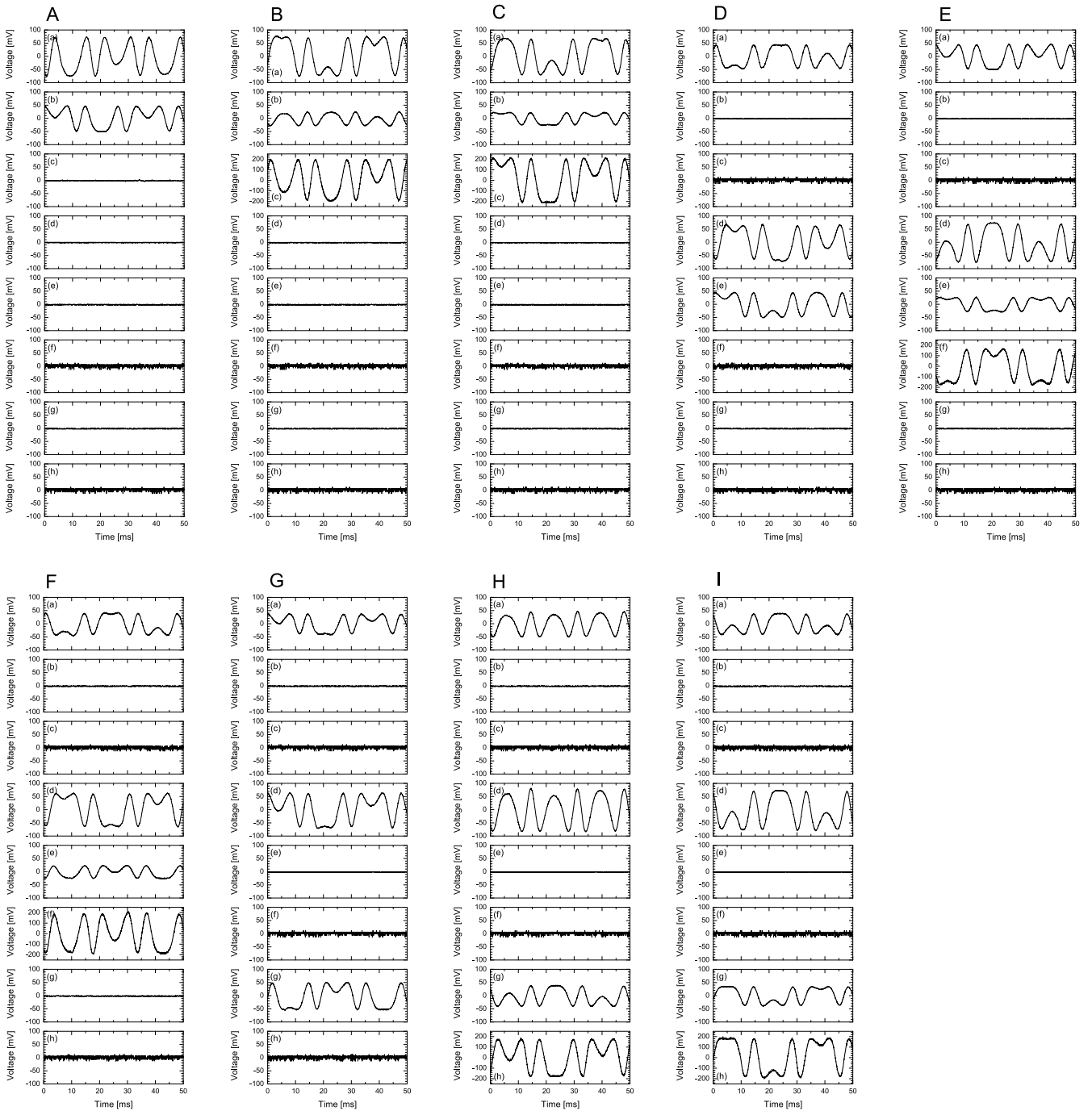

FIG. 1: Results of error syndrome measurements. A-I correspond to the cases of an error in quantum channels 1-9, respectively. (a)-(h) correspond to outputs from homodyne detectors 1-8, respectively.

APPENDIX E: THE ROLE OF MULTIPARTITE ENTANGLEMENT

The encoded nine-mode state, as created in the current experiment and described by eqs. (A1), approaches the following state in the limit of infinite squeezing,

$$|\psi_{\rm encode}\rangle = \frac{1}{\pi^{3/2}} \int dp\ dp_1\, dp_2\, dp_3\, \bar{\psi}(p)\, e^{-2ip(p_1+p_2+p_3)} \times |p_1, p_1, p_1, p_2, p_2, p_2, p_3, p_3, p_3\rangle. \quad \text{(E1)}$$

Clearly, even for infinite squeezing and perfect encoding, the inseparability properties of the total nine-party

DOI: 10.1038/NPHYS1309

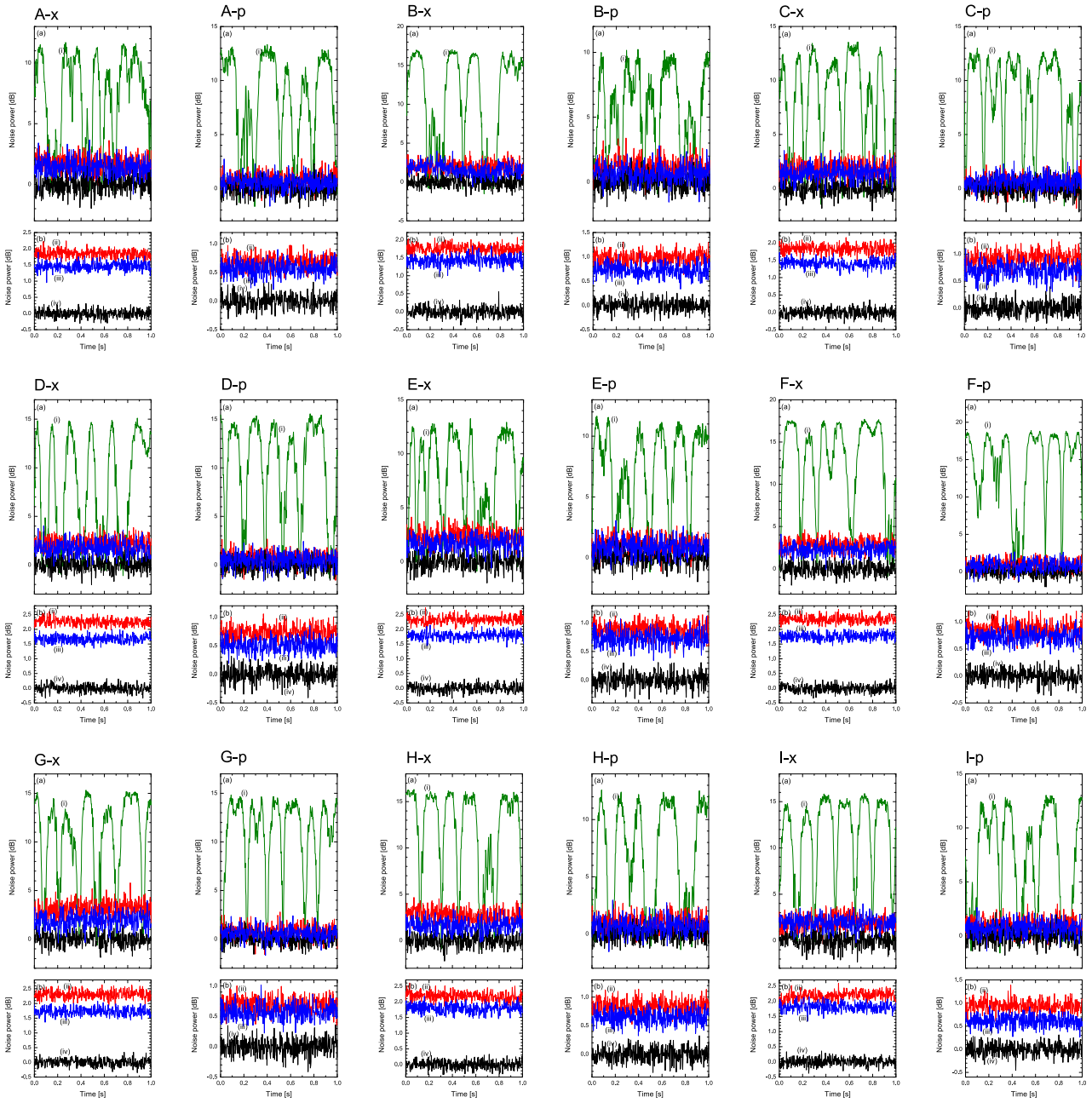

FIG. 2: Results of error correction. A-I correspond to the cases of an error in quantum channels 1-9, respectively. The LO phase of the homodyne detector is locked at x or p, which is indicated after the capital letters. Trace numbers are the same as in Figs. (5) and (6) in the main body of the paper.

state depend on the signal input wave function $\bar{\psi}(p)$. In particular, for $\bar{\psi}(p) \equiv \delta(p)$, we obtain $|\psi_{\text{encode}}\rangle = \int dp\,|p,p,p\rangle \otimes \int dp\,|p,p,p\rangle \otimes \int dp\,|p,p,p\rangle$, which is clearly not fully nine-party entangled, but rather a product state of three fully tripartite entangled GHZ-type three-mode states. So in order to obtain full nine-party entanglement, the input state should not correspond to an infinitely x-squeezed state (corresponding, after Fourier transform, to $\bar{\psi}(p) \equiv \delta(p)$). Similarly, an infinitely p-squeezed input state leads to vanishing GHZ-type correlations *within* each of the three triplets, but it has excellent GHZ-type correlations *between* the three triplets. For an input state between these two extremes, for instance, a vacuum input state as used in the experiment, we obtain quadrature correlations of both types, potentially leading to full nine-party entanglement.

In order to witness full nine-party entanglement, in addition to the correlations of eqs. (A3), p-correlations *be-*

tween the triplets and x-correlations *within* each triplet are required. Equations (A3) only describe x-correlations between the triplets and p-correlations within each triplet. The missing correlations are of the type of $\hat{p}_1+\hat{p}_4+\hat{p}_7\rightarrow 0$ and $\hat{x}_1+\hat{x}_2+\hat{x}_3\rightarrow 0$. These linear combinations correspond to the "logical" quadratures in the code space,

$$\begin{aligned}\hat{X} &\equiv \hat{x}_1+\hat{x}_2+\hat{x}_3=\hat{x}_{\rm in}+\sqrt{2}\hat{x}^{(0)}_{\rm an1}e^{-r_1}\,,\\ \hat{P} &\equiv \hat{p}_1+\hat{p}_4+\hat{p}_7=\hat{p}_{\rm in}+\sqrt{\frac{2}{3}}\hat{p}^{(0)}_{\rm an2}e^{-r_2}\\ &\quad+\sqrt{\frac{2}{3}}\hat{p}^{(0)}_{\rm an5}e^{-r_5}+\sqrt{\frac{2}{3}}\hat{p}^{(0)}_{\rm an7}e^{-r_7}\,,\end{aligned}\tag{E2}$$

obviously depending on the signal input state. Only for infinite ancilla squeezing, the encoding is perfect, $\hat{X}=\hat{x}_{\rm in}$ and $\hat{P}=\hat{p}_{\rm in}$. The excess noise in each quadrature is $2\times e^{-2r}/4$ for equal squeezing of the ancilla modes. In this case, an infinitely x-squeezed input state would lead to excellent intra-triplet x-correlations; an infinitely p-squeezed input state, favorable for good inter-triplet p-correlations, leads to vanishing intra-triplet x-correlations. With a vacuum input state, as used in the experiment, we have both types of quantum correlations for nonzero squeezing of the ancilla modes. Similar quantum correlations also exist for the combinations

$$\begin{aligned}\hat{x}_4+\hat{x}_5+\hat{x}_6 &= \hat{x}_{\rm in}-\frac{1}{\sqrt{2}}\hat{x}^{(0)}_{\rm an1}e^{-r_1}+\sqrt{\frac{3}{2}}\hat{x}^{(0)}_{\rm an4}e^{-r_4}\,,\\ \hat{x}_7+\hat{x}_8+\hat{x}_9 &= \hat{x}_{\rm in}-\frac{1}{\sqrt{2}}\hat{x}^{(0)}_{\rm an1}e^{-r_1}-\sqrt{\frac{3}{2}}\hat{x}^{(0)}_{\rm an4}e^{-r_4}\,,\\ \hat{p}_2+\hat{p}_5+\hat{p}_8 &= \hat{p}_{\rm in}-\frac{1}{\sqrt{6}}\hat{p}^{(0)}_{\rm an2}e^{-r_2}+\sqrt{\frac{1}{2}}\hat{p}^{(0)}_{\rm an3}e^{-r_3}\\ &\quad-\frac{1}{\sqrt{6}}\hat{p}^{(0)}_{\rm an5}e^{-r_5}+\sqrt{\frac{1}{2}}\hat{p}^{(0)}_{\rm an6}e^{-r_6}\\ &\quad-\frac{1}{\sqrt{6}}\hat{p}^{(0)}_{\rm an7}e^{-r_7}+\sqrt{\frac{1}{2}}\hat{p}^{(0)}_{\rm an8}e^{-r_8}\,,\\ \hat{p}_3+\hat{p}_6+\hat{p}_9 &= \hat{p}_{\rm in}-\frac{1}{\sqrt{6}}\hat{p}^{(0)}_{\rm an2}e^{-r_2}-\sqrt{\frac{1}{2}}\hat{p}^{(0)}_{\rm an3}e^{-r_3}\\ &\quad-\frac{1}{\sqrt{6}}\hat{p}^{(0)}_{\rm an5}e^{-r_5}-\sqrt{\frac{1}{2}}\hat{p}^{(0)}_{\rm an6}e^{-r_6}\\ &\quad-\frac{1}{\sqrt{6}}\hat{p}^{(0)}_{\rm an7}e^{-r_7}-\sqrt{\frac{1}{2}}\hat{p}^{(0)}_{\rm an8}e^{-r_8}\,.\end{aligned}\tag{E3}$$

The total set of quadrature quantum correlations can be sufficient for a fully inseparable nine-party entangled state. The corresponding nine-party entanglement witnesses lead to the known criteria for multi-party inseparability of continuous-variable states[1]. In order to verify three-party inseparability within each triplet $\hat{\rho}_{123}$, $\hat{\rho}_{456}$, and $\hat{\rho}_{789}$, we have, for $\hat{\rho}_{123}$,

$$\begin{aligned}&\langle[\Delta(\hat{p}_1-\hat{p}_2)]^2\rangle+\langle[\Delta(\hat{x}_1+\hat{x}_2+g_{1a}\,\hat{x}_3)]^2\rangle<1,\\ &\langle[\Delta(\hat{p}_2-\hat{p}_3)]^2\rangle+\langle[\Delta(g_{1b}\,\hat{x}_1+\hat{x}_2+\hat{x}_3)]^2\rangle<1,\end{aligned}\tag{E4}$$

for $\hat{\rho}_{456}$,

$$\begin{aligned}&\langle[\Delta(\hat{p}_4-\hat{p}_5)]^2\rangle+\langle[\Delta(\hat{x}_4+\hat{x}_5+g_{2a}\,\hat{x}_6)]^2\rangle<1,\\ &\langle[\Delta(\hat{p}_5-\hat{p}_6)]^2\rangle+\langle[\Delta(g_{2b}\,\hat{x}_4+\hat{x}_5+\hat{x}_6)]^2\rangle<1,\end{aligned}\tag{E5}$$

for $\hat{\rho}_{789}$,

$$\begin{aligned}&\langle[\Delta(\hat{p}_7-\hat{p}_8)]^2\rangle+\langle[\Delta(\hat{x}_7+\hat{x}_8+g_{3a}\,\hat{x}_9)]^2\rangle<1,\\ &\langle[\Delta(\hat{p}_8-\hat{p}_9)]^2\rangle+\langle[\Delta(g_{3b}\,\hat{x}_7+\hat{x}_8+\hat{x}_9)]^2\rangle<1.\end{aligned}\tag{E6}$$

The "gains" g_{1a}, etc., can be used to optimize these conditions. In order to rule out a state of the form $\sum_i\eta_i\hat{\rho}^{(i)}_{123}\otimes\hat{\rho}^{(i)}_{456}\otimes\hat{\rho}^{(i)}_{789}\equiv\sum_i\eta_i\hat{\rho}^{(i)}_a\otimes\hat{\rho}^{(i)}_b\otimes\hat{\rho}^{(i)}_c$, we need further criteria, for example,

$$\begin{aligned}&\langle[\Delta(\hat{p}_1+\hat{p}_4+g_{11}\,\hat{p}_7)]^2\rangle\\ &+\langle[\Delta(\hat{x}_1+g_{12}\,\hat{x}_2+g_{13}\,\hat{x}_3-\hat{x}_4-g_{14}\,\hat{x}_5-g_{15}\,\hat{x}_6)]^2\rangle<1,\end{aligned}\tag{E7}$$

$$\begin{aligned}&\langle[\Delta(g_{21}\,\hat{p}_1+\hat{p}_4+\hat{p}_7)]^2\rangle\\ &+\langle[\Delta(\hat{x}_4+g_{22}\,\hat{x}_5+g_{23}\,\hat{x}_6-\hat{x}_7-g_{24}\,\hat{x}_8-g_{25}\,\hat{x}_9)]^2\rangle<1,\end{aligned}\tag{E8}$$

which describe the inter-triplet correlations. Equation (E7) rules out the forms $\sum_i\eta_i\hat{\rho}^{(i)}_a\otimes\hat{\rho}^{(i)}_{bc}$ and $\sum_i\eta_i\hat{\rho}^{(i)}_b\otimes\hat{\rho}^{(i)}_{ac}$; eq. (E8) rules out the forms $\sum_i\eta_i\hat{\rho}^{(i)}_c\otimes\hat{\rho}^{(i)}_{ab}$ and $\sum_i\eta_i\hat{\rho}^{(i)}_b\otimes\hat{\rho}^{(i)}_{ac}$. Thus, any form of separability between the triplets a, b, and c can be ruled out. The inter-triplet conditions can be understood as GHZ-type correlations of modes 1, 4, and 7 after LOCC operations; namely, x-measurements of modes 2, 3, 5, 6, 8, 9 and the corresponding displacements of modes 1, 4, and 7.

In the experiment, it was verified that in any of the nine cases of an error in any one of the nine channels, the classical cutoff (zero-squeezing limit) was exceeded. This confirms that all 8 ancilla modes are in a squeezed state (see Table 1 and Fig.2), as the quadrature noise of every ancilla mode contributes to the excess noise of the corrected signal for some of the detector results used for feedforward. This squeezing translates into nonclassical correlations for all combinations in eqs. (A2), (E2), and (E3) (with a vacuum input state). The set of quadrature combinations corresponds to the "unit-gain" version of the entanglement witnesses in eqs. (E4), (E5), (E6), (E7), and (E8). In order to satisfy the witness inequalities, in particular, for small squeezing values (as those of roughly 1 dB in the experiment), non-unit gain must be chosen. Although these non-unit gain combinations have not been measured directly in the quantum error correction experiment, the nonclassicality in *all* the unit-gain combinations may be interpreted as an indirect confirmation of the presence of nine-party entanglement.

DOI: 10.1038/NPHYS1309

APPENDIX F: APPLICABILITY OF CONTINUOUS-VARIABLE CODES

The continuous-variable nine-mode code corrects an arbitrary error occurring in *any one* of the nine channels. Similar to the qubit case, for realistic scenarios, we should consider imperfect transmissions in *every* channel under the reasonable assumption of errors acting independently in all the channels. The performance of the code can then be evaluated by comparing the transfer fidelities for the encoded scheme with a direct transmission of the signal state through a single noisy channel[2].

Using the example of a 3-wavepacket code, we shall demonstrate that for certain stochastic error models, the continuous-variable code leads to a dramatic improvement of fidelity even when the errors occur in every channel[3]. In this case, the errors should correspond to x-displacements or any errors decomposable into x-displacements (including non-Gaussian "x-errors"). A code for correcting arbitrary errors including non-commuting x and p-errors is obtainable, for instance, by concatenating the 3-mode code into a 9-mode code, as implemented in the current experiment. The appropriate error models are reminiscent of the most typical qubit channels such as bit-flip and phase-flip channels. In the continuous-variable regime, these types of stochastic errors would map a Gaussian signal state into a non-Gaussian state represented by a discrete, incoherent mixture of the input state with a Gaussian (or even a non-Gaussian) state,

$$W_{\rm out}(x,p) = (1-\gamma)W_{\rm in} + \gamma W_{\rm error}\,. \tag{F1}$$

Here, the input state described by the Wigner function $W_{\rm in}$ is transformed into a new state $W_{\rm error}$ with probability γ; it remains unchanged with probability $1-\gamma$. A special case of the above channel model is an erasure channel[4]. The generalized erasure model here may find applications in free-space communication with fluctuating losses and beam point jitter effects[5–7].

As an example, we will consider a coherent-state input, $|\bar{\alpha}_1\rangle = |\bar{x}_1 + i\bar{p}_1\rangle$, described by the Wigner function,

$$W_{\rm in}(x_1,p_1) = \frac{2}{\pi}\exp[-2(x_1-\bar{x}_1)^2 - 2(p_1-\bar{p}_1)^2]\,. \tag{F2}$$

Moreover, we assume that the effect of the error is just an x-displacement by $\bar{x}_2$ such that

$$W_{\rm error}(x_1,p_1) = W_{\rm in}(x_1-\bar{x}_2,p_1)\,. \tag{F3}$$

The sign of the displacement error shall be fixed and known, $\bar{x}_2 > 0$.

Now in order to encode the input state, we use two ancilla modes, each in a single-mode x-squeezed vacuum state, represented by

$$W_{\rm anc}(x_k,p_k) = \frac{2}{\pi}\exp[-2e^{+2r}x_k^2 - 2e^{-2r}p_k^2]\,, \tag{F4}$$

with squeezing parameter r and $k = 2,3$. The total three-mode state before encoding is

$$W(\alpha_1,\alpha_2,\alpha_3) = W_{\rm in}(x_1,p_1)W_{\rm anc}(x_2,p_2)W_{\rm anc}(x_3,p_3), \tag{F5}$$

with $\alpha_j = x_j + ip_j$, $j = 1,2,3$. The encoding may be achieved by applying a "tritter", i.e., a sequence of two beam splitters with transmittances $1:2$ and $1:1$. The total, encoded state will be an entangled three-mode Gaussian state with Wigner function,

$$\begin{aligned} W_{\rm enc}(\alpha_1,\alpha_2,\alpha_3) &= \left(\frac{2}{\pi}\right)^3 \\ &\times \exp\Big\{-2\Big[\frac{1}{\sqrt{3}}\Big(x_1+x_2+x_3\Big)-\bar{x}_1\Big]^2 \\ &\quad -\frac{2}{3}e^{-2r}\Big[(p_1-p_2)^2+(p_2-p_3)^2+(p_1-p_3)^2\Big] \\ &\quad -2\Big[\frac{1}{\sqrt{3}}\Big(p_1+p_2+p_3\Big)-\bar{p}_1\Big]^2 \\ &\quad -\frac{2}{3}e^{+2r}\Big[(x_1-x_2)^2+(x_2-x_3)^2+(x_1-x_3)^2\Big]\Big\}. \end{aligned} \tag{F6}$$

Now we send the three modes through individual channels where each channel acts independently upon *every* mode as described by Eq. (F1) with $W_{\rm error}$ corresponding to an x-displacement by $\bar{x}_2$. As a result, the three noisy channels will turn the encoded state into the following three-mode state,

$$\begin{aligned} &W'_{\rm enc}(\alpha_1,\alpha_2,\alpha_3) \\ &= (1-\gamma)^3 W_{\rm enc}(\alpha_1,\alpha_2,\alpha_3) \\ &\quad +\gamma(1-\gamma)^2 W_{\rm enc}(x_1-\bar{x}_2+ip_1,\alpha_2,\alpha_3) \\ &\quad +\gamma(1-\gamma)^2 W_{\rm enc}(\alpha_1,x_2-\bar{x}_2+ip_2,\alpha_3) \\ &\quad +\gamma(1-\gamma)^2 W_{\rm enc}(\alpha_1,\alpha_2,x_3-\bar{x}_2+ip_3) \\ &\quad +\gamma^2(1-\gamma) W_{\rm enc}(x_1-\bar{x}_2+ip_1,x_2-\bar{x}_2+ip_2,\alpha_3) \\ &\quad +\gamma^2(1-\gamma) W_{\rm enc}(x_1-\bar{x}_2+ip_1,\alpha_2,x_3-\bar{x}_2+ip_3) \\ &\quad +\gamma^2(1-\gamma) W_{\rm enc}(\alpha_1,x_2-\bar{x}_2+ip_2,x_3-\bar{x}_2+ip_3) \\ &\quad +\gamma^3 W_{\rm enc}(x_1-\bar{x}_2+ip_1,x_2-\bar{x}_2+ip_2,x_3-\bar{x}_2+ip_3). \end{aligned} \tag{F7}$$

The decoding procedure now simply means inverting the tritter, which results in

$$\begin{aligned} &W_{\rm dec}(\alpha_1,\alpha_2,\alpha_3) \\ &= (1-\gamma)^3 W_{\rm in}(x_1,p_1)W_{\rm anc}(x_2,p_2)W_{\rm anc}(x_3,p_3) \\ &\quad +\gamma(1-\gamma)^2 W_{\rm in}\left(x_1-\frac{1}{\sqrt{3}}\bar{x}_2,p_1\right) \\ &\qquad \times W_{\rm anc}\left(x_2-\sqrt{\frac{2}{3}}\bar{x}_2,p_2\right)W_{\rm anc}(x_3,p_3) \\ &\quad +\gamma(1-\gamma)^2 W_{\rm in}\left(x_1-\frac{1}{\sqrt{3}}\bar{x}_2,p_1\right) \\ &\qquad \times W_{\rm anc}\left(x_2+\frac{1}{\sqrt{6}}\bar{x}_2,p_2\right)W_{\rm anc}(x_3-\frac{1}{\sqrt{2}}\bar{x}_2,p_3) \end{aligned} \tag{F8}$$

$$
\begin{aligned}
&+\gamma(1-\gamma)^2 W_{\rm in}\left(x_1-\frac{1}{\sqrt{3}}\bar{x}_2,p_1\right)\\
&\quad\times W_{\rm anc}\left(x_2+\frac{1}{\sqrt{6}}\bar{x}_2,p_2\right)W_{\rm anc}(x_3+\frac{1}{\sqrt{2}}\bar{x}_2,p_3)\\
&+\gamma^2(1-\gamma)W_{\rm in}\left(x_1-\frac{2}{\sqrt{3}}\bar{x}_2,p_1\right)\\
&\quad\times W_{\rm anc}\left(x_2-\frac{1}{\sqrt{6}}\bar{x}_2,p_2\right)W_{\rm anc}(x_3-\frac{1}{\sqrt{2}}\bar{x}_2,p_3)\\
&+\gamma^2(1-\gamma)W_{\rm in}\left(x_1-\frac{2}{\sqrt{3}}\bar{x}_2,p_1\right)\\
&\quad\times W_{\rm anc}\left(x_2-\frac{1}{\sqrt{6}}\bar{x}_2,p_2\right)W_{\rm anc}(x_3+\frac{1}{\sqrt{2}}\bar{x}_2,p_3)\\
&+\gamma^2(1-\gamma)W_{\rm in}\left(x_1-\frac{2}{\sqrt{3}}\bar{x}_2,p_1\right)\\
&\quad\times W_{\rm anc}\left(x_2+\sqrt{\frac{2}{3}}\bar{x}_2,p_2\right)W_{\rm anc}(x_3,p_3)\\
&+\gamma^3 W_{\rm in}\left(x_1-\sqrt{3}\bar{x}_2,p_1\right)\\
&\quad\times W_{\rm anc}\left(x_2,p_2\right)W_{\rm anc}(x_3,p_3).
\end{aligned}
$$

By looking at this state, we can easily see that x-homodyne detections of the ancilla modes 2 and 3 (the syndrome measurements) will almost unambiguously identify in which channel a displacement error occurred and how many modes were subject to a displacement error. The only ambiguity comes from the case of an error occurring in every channel at the same time (with probability γ^3), which is indistinguishable from the case where no error at all happens. In both cases, the two ancilla modes are transformed via decoding back into the two initial single-mode squeezed vacuum states. All the other cases, however, can be identified, provided the initial squeezing r is sufficiently large such that the displacements $\propto \bar{x}_2$, originating from the errors, can be resolved in the ancilla states.

The recovery operation, i.e., the final phase-space displacement of mode 1 depends on the syndrome measurement results for modes 2 and 3 which are consistent with either undisplaced squeezed vacuum states ('0') or squeezed vacua displaced in either '+' or '−' x-direction. The syndrome results for modes 2 and 3 corresponding to the eight possibilities for the errors occurring in the three channels are (0,0) for no error at all, (+,0) for an error in channel 1, (−,+) for an error in channel 2, (−,−) for an error in channel 3, (+,+) for errors in channels 1 and 2, (+,−) for errors in channels 1 and 3, (−,0) for errors in channels 2 and 3, and, again, (0,0) for errors occurring in all three channels.

In the limit of infinite squeezing of the ancilla modes, the ensemble output state of mode 1 (upon averaging over all syndrome measurement results x_2 and x_3 including suitable feedforward operations) can be described as

$$
(1-\gamma^3)W_{\rm in}(x_1,p_1)+\gamma^3 W_{\rm in}\left(x_1-\sqrt{3}\bar{x}_2,p_1\right). \quad \text{(F9)}
$$

This output state emerges, because in almost all cases, the feedforward operations turn mode 1 back into the initial state (in the case of finite squeezing, only up to some Gaussian-distributed excess noise depending on the degree of squeezing used for the encoding). The only case for which no correction occurs is when errors appear in every channel at the same time, at a probability of γ^3. In this case, the initial state remains uncorrected, with an x-displacement error of $\sqrt{3}\bar{x}_2$.

We see that a fidelity of $1-\gamma^3$ can be achieved, assuming $\bar{x}_2 \gg 1$ (for smaller $\bar{x}_2$, the fidelity would even exceed $1-\gamma^3$, but those smaller $\bar{x}_2$ may be too hard to detect at the syndrome extraction, depending on the degree of squeezing, see below). Note that this result implies that the encoded scheme performs better than the unencoded scheme (direct transmission with $F_{\rm direct}=1-\gamma$) for *any* $0<\gamma<1$. In other words, by employing the quantum error correction protocol, the error probability can be reduced from γ to γ^3. The continuous-variable scheme in this model is more efficient than the analogous qubit repetition code and it does not require error probabilities $\gamma<1/2$ as for the case of qubit bit-flip errors[2].

We may consider two different regimes for the error displacements $\bar{x}_2$. First, the regime $e^{-2r}/4<\bar{x}_2<1/4$, corresponding to small displacements below the shot noise limit; these can only be resolved provided the squeezing is large enough. In the limit of infinite squeezing $r\to\infty$, arbitrarily small shifts can be detected and perfectly corrected (with zero excess noise in the output states corresponding to unit fidelity).

Secondly, the regime $\bar{x}_2 \gg 1$. For these large shifts, even zero squeezing in the ancilla modes (i.e., vacuum ancilla states) is sufficient for error identification. Even with $r=0$, the syndrome measurements still provide enough information on the location of the error and, to some extent, on the size of the error. We may refer to this kind of scheme as quantum-limited error correction (QLEC), corresponding to the "classical" cutoff used as a classical/quantum boundary in the main body of the paper. This classical cutoff depends on the particular encoding and decoding circuit used; in the experiment, it is the same circuit as that employed for quantum error correction (neither of these are necessarily optimal).

QLEC for large shifts $\bar{x}_2 \gg 1$ (the regime of the experiment) works fairly well. In fact, the fidelity values without QLEC drop to near-zero fidelities, as measured in the experiment, $F<0.007\pm0.001$. Experimentally, this QLEC is a highly nontrivial task and it is needed to achieve reasonable transfer fidelities (this is similar to the classical/quantum fidelity benchmarks for continuous-variable teleportation which are not near zero, but rather at values such as 1/2 with coherent input states[8,9]). Nonetheless, the QLEC scheme results in excess noise for the output state coming from the feedforward operations based on the fluctuating syndrome measurement results. By employing squeezed-state ancilla modes, this excess noise can be reduced (down to zero for infinite squeezing). In this case, the scheme operates

DOI: 10.1038/NPHYS1309

in the quantum regime. Significantly, in the experiment, non-commuting errors have been corrected, which means that QLEC will always result in some excess noise. Although the margin of the demonstrated quantum error correction (on top of the QLEC) is rather small, the experimental data provide clear evidence that QLEC has been outperformed by the quantum scheme.

[1] P. van Loock and A. Furusawa, Phys. Rev. A **67**, 052315 (2003).
[2] M. A. Nielsen and I. L. Chuang, *Quantum Computation and Quantum Information* (Cambridge University Press, 2000).
[3] P. van Loock, *Los Alamos arXiv*, quant-ph/0811.3616 (2008).
[4] J. Niset et al., Phys. Rev. Lett. **101**, 130503 (2008).
[5] J. Heersink et al., Phys. Rev. Lett. **96**, 235601 (2006).
[6] R. Dong et al., Nature Physics **4**, 919-923 (2008).
[7] B. Hage et al., Nature Physics **4**, 915-918 (2008).
[8] S. L. Braunstein et al., Phys. Rev. A **64**, 022321 (2001).
[9] K. Hammerer et al., Phys. Rev. Lett. **94**, 150503 (2005).